

SUPPLEMENTAL MATERIAL AND METHODS

Casparian strip visualization.

After immunolocalization of MtNramp1-HA in roots and subsequent analysis by confocal microscopy, these sections were stained using the berberine-aniline blue method (Brundrett et al., 1988). Briefly, sections were incubated with 0.1% berberine hemi-sulphate (Sigma) in water for 1 h. After washing with water, samples were incubated in 0.5% aniline blue in water for 30 min and then rinsed with water. Finally, sections were transferred to 0.1% FeCl₃ in 50% glycerol for several minutes and mounted in the same solution. Images were obtained using a confocal laser-scanning microscope (Leica SP8, Wetzlar, Germany).

Iron distribution visualization

Roots and nodules from 28 dpi wild type and *nramp1-1* plants were collected and fixed in 0.25% glutaraldehyde, 4% formaldehyde, 2.5% sucrose in 50 mM potassium phosphate buffer (pH 7.4) at 4 °C overnight. Samples were then dehydrated using ethanol series and embedded in LR-White resin (London Resin Company Ltd, UK) (Rodríguez-Haas et al., 2013). Finally, nodules were placed in gelatine capsules, filled with resin and polymerized at 60°C for 24 h. Serial thin sections (1µm) were cut with a Reichert Ultracut S ultramicrotome (Leica, Vienna, Austria) fitted with a diamond knife. Sections for nodule structure analysis were stained with a mixture of 1% (w/v) toluidine blue in aqueous 1% sodium borate and 1% (w/v) methylene blue in water. Iron distribution was visualized using the Perl-DAB method (Roschttardt et al., 2009). Direct observation of sections was performed under a Zeiss Axiophot photomicroscope (Carl Zeiss, Oberkochen, Germany) with an attached digital camera (Leica DFC 420C, Heerburgg, Switzerland). A minimum of three nodules and roots per treatment and three sections per sample were examined.

Brundrett M, Enstone D, Peterson C (1988) A berberine-aniline blue fluorescent staining procedure for suberin, lignin, and callose in plant tissue. *Protoplasma* **146**: 133-142

Rodríguez-Haas B, Finney L, Vogt S, González-Melendi P, Imperial J, González-Guerrero M (2013) Iron distribution through the developmental stages of *Medicago truncatula* nodules. *Metallomics* **5**: 1247-1253

Roschztardt H, Conejero G, Curie C, Mari S (2009) Identification of the endodermal vacuole as the iron storage compartment in the Arabidopsis embryo. *Plant Physiol* **151**: 1329-1338

SUPPLEMENTAL FIGURE LEGENDS

Supplemental Figure S1. *MtNramp* gene family expression. Gene expression of the corresponding *MtNramp* gene in nitrogen-fertilized roots (NFR), denodulated roots (DR) and nodules (Nod) relative to the internal standard gene *ubiquitin carboxyl-terminal hydrolase*. Data are the mean \pm SE of three independent experiments.

Supplemental Figure S2. *MtNramp1*-HA yeast complementation assay. Yeast strain BY4741 was transformed with the pYPGE15 empty vector, while BY4741-derived BR4742 strain mutated in *smf1* was transformed with either pYPGE15 alone, or with pYPEG15 containing *MtNramp1* CDS, or with pYPGE15 harbouring *MtNramp1* CDS with a C-terminal 3xHA tag. Serial dilutions (10x) of each transformant were grown for 3 days at 30°C on SD Glucose media with all the required amino acids. pH was buffered with 50 mM MES and Mn levels were kept low with 6.25 mM EGTA. Mn-replete positive controls were obtained by supplementing the plate with 500 μ M MnSO₄.

Supplemental Figure S3. Antibody-specificity control for immunolocalization. Cross section of a 28 dpi *M. truncatula* nodule infected with *S. meliloti* constitutively expressing GFP (green) and transformed with a vector expressing *MtNramp1* under the regulation of its endogenous promoter. MtNramp1 localization was determined using an Alexa 594-conjugated antibody (red). DNA was stained with DAPI (blue). Infection threads are indicated with asterisks. Scale bar represents 100 μ m.

Supplemental Figure S4. Expression in the different *M. truncatula* nodule zones. (A) *MtNramp1*. (B) Nodule-specific MATE transporter *Medtr6g081400*. ZI indicates zone I; ZII_d, distal zone II (region closest to zone I); ZII_p, proximal zone II; IZ is the interzone between zone II and zone III; and ZIII, zone III. Data were obtained from the Symbimics database (<https://iant.toulouse.inra.fr/symbimics>).

Supplemental Figure S5. MtNramp1-HA localization in the root. (A) Confocal microscopy localization of MtNramp1-HA in a cross section of a 28 dpi *M. truncatula* root transformed with a vector expressing *MtNramp1* under the regulation of its endogenous promoter. MtNramp1 position was determined using an Alexa 594-

conjugated antibody (red). DNA and xylem was stained with DAPI (blue). (B) Bright-field image of the cross section. (C) Overlay of panels A and B. (D) Close-up of overlaid MtNramp1-HA localization in *M. truncatula* transformed roots (detected with an Alexa 594-conjugated antibody in red) and bright-field image. (E) Casparian strip localization (blue) detected with the berberine-aniline blue method. (F) Overlay of panels D and E. Scale bars represent 50 μm (panels A-C) or 10 μm (panels D-F).

Supplemental Figure S6. Phenotype of *nramp1-1* under non-symbiotic conditions.

(A) Growth of representative plants. Scale bar represents 1 cm. Fe concentrations in nutritive solutions used are indicated below. (B) Fresh weight of shoots and roots. Data are the mean \pm SE (n = 5 plants). (C) Chlorophyll content. Data are the mean \pm SE (n = 3 plants). (D) Iron content in roots and shoots of wild-type and *nramp1-1* plants under two different iron fertilization levels. Data are the mean \pm SE of two sets of five pooled plants. * indicates significant differences ($p \leq 0.05$). (E) *MtFRO1* expression in wild type and *nramp1-1* plants under two different iron fertilization levels. Data are the mean \pm SE of three independent experiments. * indicates significant differences ($p \leq 0.05$).

Supplemental Figure S7. Iron complementation of *nramp1-1* phenotype.

(A) Growth of representative plants. Scale bar represents 1 cm. (B) Fresh weight of shoots and roots. Data are the mean \pm SE (n = 8 plants). (C) Nodule number per plant. 100 % = 4.25 nodules/plant. Data are the average \pm SE (n=8-10 plants). (D) Nitrogenase activity in 28 dpi nodules. Acetylene reduction was measured in duplicate from two sets of five pooled plants. Data are the mean \pm SE. 100% = 61.17 nmol ethylene $\text{h}^{-1}\text{g}^{-1}$.

Supplemental Figure S8. Iron distribution in roots and nodules of wild type and *nramp1-1* plants.

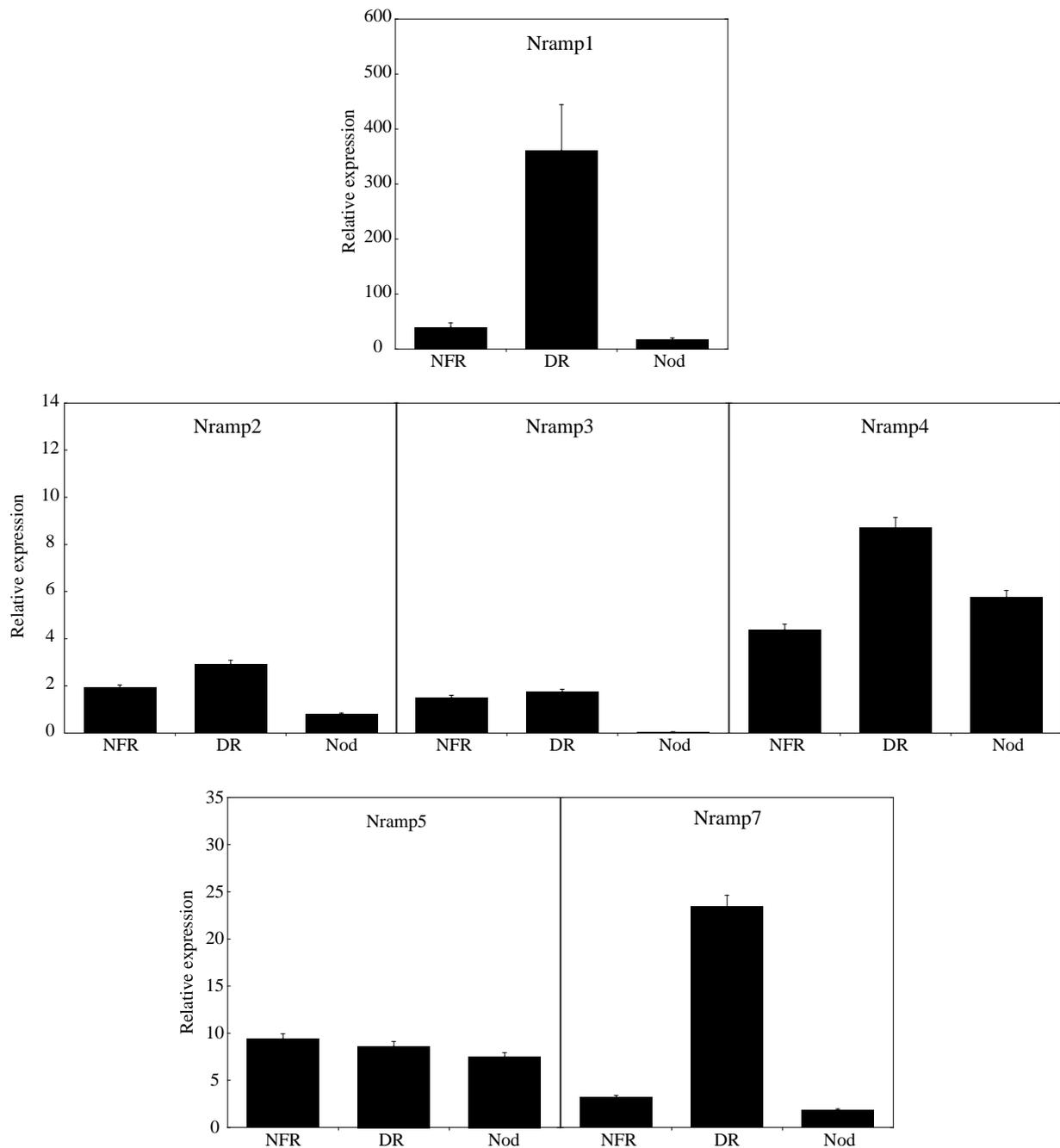
(A) wild type *M. truncatula* nodule and (B) *nramp1-1* *M. truncatula* nodule. Left panels show reference sections stained with toluidine blue and methylene blue, the boxed regions represent the approximate area corresponding to the Perl-DAB-stained (right panel) which shows the iron distribution. Nodule zones are indicated. (C) Iron distribution in wild type *M. truncatula* root. Left panel shows a root section stained with toluidine blue and methylene blue, the boxed region represents the approximate area corresponding to the Perl-DAB-stained right panel. (D) Iron distribution in *nramp1-1* *M. truncatula* root. Left panel shows a reference section stained with toluidine blue and methylene blue, the boxed region represents the approximate area

corresponding to the Perl-DAB-stained right panel. Arrowheads indicate regions of iron accumulation. (E) Close-up view of Perl-DAB stained *nramp1-1* root (corresponding to the boxed area of the right panel in D). Arrowheads indicate regions of iron accumulation. Scale bars represent 100 μm (A-C, and left panel D), 50 μm (right panel D), or 10 μm (E).

Supplemental Figure S9. Non-symbiotic phenotype *nramp1-1* under Mn deficiency conditions. (A) Growth of representative plants. Scale bar represents 1 cm. Manganese concentrations in nutritive solutions used are indicated below. (B) Fresh weight of shoots and roots. Data are the mean \pm SE (n = 5 plants). (C) Chlorophyll content. Data are the mean \pm SE (n = 3 plants). (D) Manganese content in roots and shoots of wild-type and *nramp1-1* plants under two different manganese fertilization levels. Data are the mean \pm SE of two sets of five pooled plants. * indicates significant differences ($p \leq 0.05$).

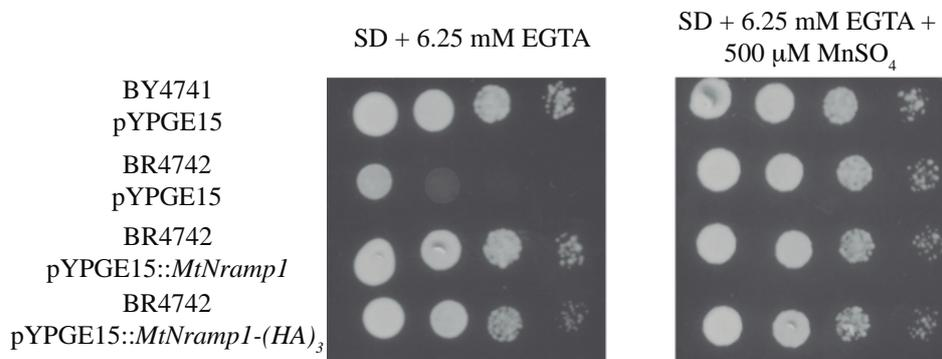
Supplemental Figure S10. Symbiotic phenotype of *nramp1-1* under two different Mn concentrations (A) Growth of representative plants. Scale bar represents 1 cm. (B) Close view of representative nodules of each *M. truncatula* line. Scale bar represents 1 mm. (C) Fresh weight of shoots and roots. Data are the mean \pm SE (n = 6-8 plants). (D) Nodule number per plant. 100 % = 4.21 nodules/plant. Data are the average \pm SE (n= 7 plants). (E) Nitrogenase activity in 28 dpi nodules. Acetylene reduction was measured in duplicate from two sets of five pooled plants. Data are the mean \pm SE. 100% = 26.69 nmol ethylene h⁻¹g⁻¹. (F) Mn content (ppm) in 28 dpi plants. Bars indicate the average \pm SE of two sets of 5 transformed plants. * indicates significant differences ($p \leq 0.05$).

SUPPLEMENTAL FIGURE S1



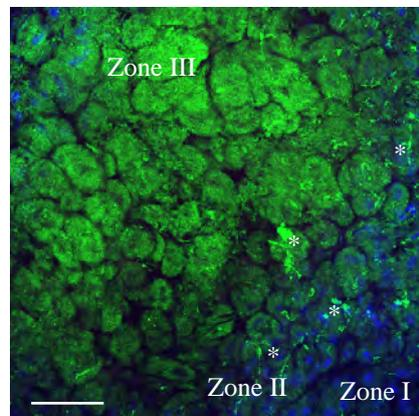
Supplemental Figure S1. *MtNramp* gene family expression. Gene expression of the corresponding *MtNramp* gene in nitrogen-fertilized roots (NFR), denodulated roots (DR) and nodules (Nod) relative to the internal standard gene *ubiquitin carboxyl-terminal hydrolase*. Data are the mean \pm SE of three independent experiments.

SUPPLEMENTAL FIGURE S2



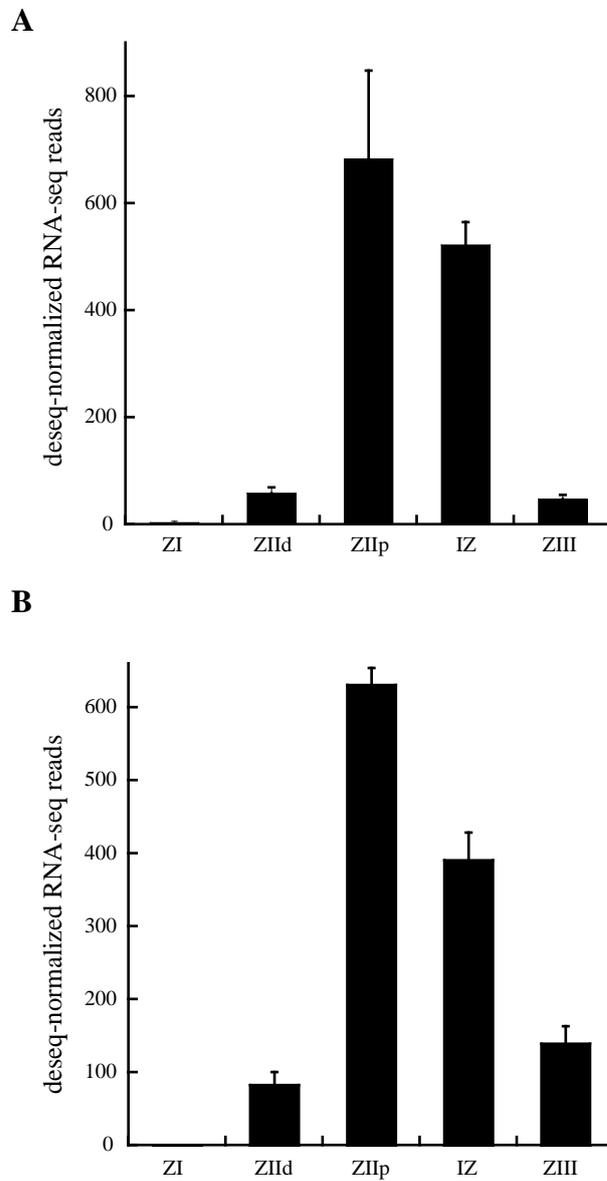
Supplemental Figure S2. *MtNramp1*-HA yeast complementation assay. Yeast strain BY4741 was transformed with the pYPGE15 empty vector, while BY4741-derived BR4742 strain mutated in *smf1* was transformed with either pYPGE15 alone, or with pYPEG15 containing *MtNramp1* CDS, or with pYPGE15 harbouring *MtNramp1* CDS with a C-terminal 3xHA tag. Serial dilutions (10x) of each transformant were grown for 3 days at 30°C on SD Glucose media with all the required amino acids. pH was buffered with 50 mM MES and Mn levels were kept low with 6.25 mM EGTA. Mn-replete positive controls were obtained by supplementing the plate with 500 μ M $MnSO_4$.

SUPPLEMENTAL FIGURE S3



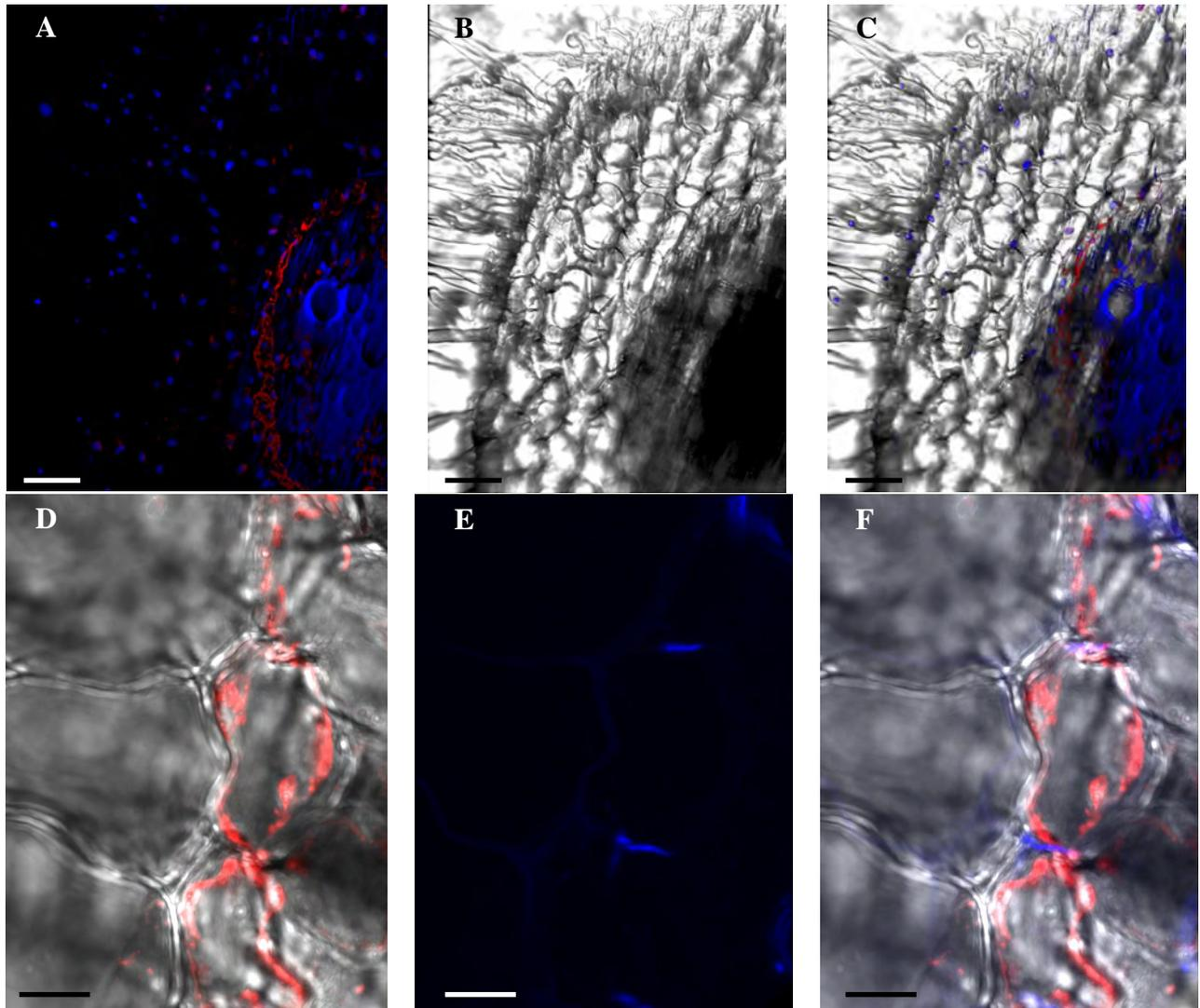
Supplemental Figure S3. Antibody-specificity control for immunolocalization. Cross section of a 28 dpi *M. truncatula* nodule infected with *S. meliloti* constitutively expressing GFP (green) and transformed with a vector expressing *MtNramp1* under the regulation of its endogenous promoter. MtNramp1 localization was determined using an Alexa 594-conjugated antibody (red). DNA was stained with DAPI (blue). Infection threads are indicated with asterisks. Scale bar represents 100 μm .

SUPPLEMENTAL FIGURE S4



Supplemental Figure S4. Expression in the different *M. truncatula* nodule zones. (A) MtNramp1. (B) Nodule-specific MATE transporter *Medtr6g081400*. ZI indicates zone I; ZII_d, distal zone II (region closest to zone I); ZII_p, proximal zone II; IZ is the interzone between zone II and zone III; and ZIII, zone III. Data were obtained from the Symbimics database (<https://iant.toulouse.inra.fr/symbimics>).

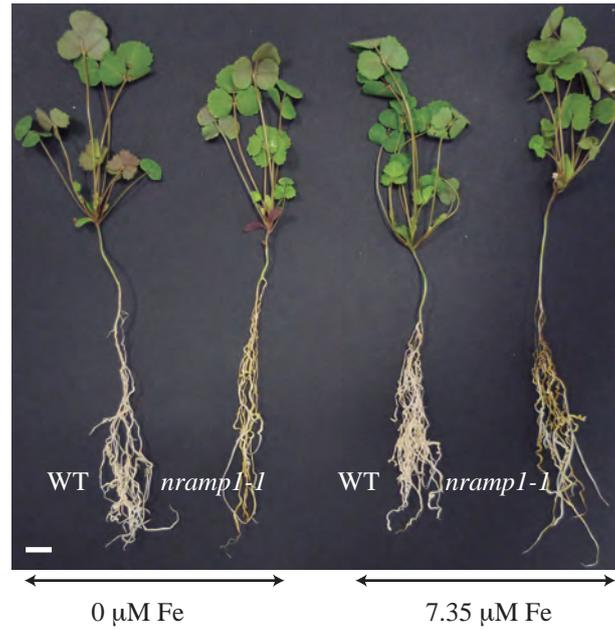
SUPPLEMENTAL FIGURE S5



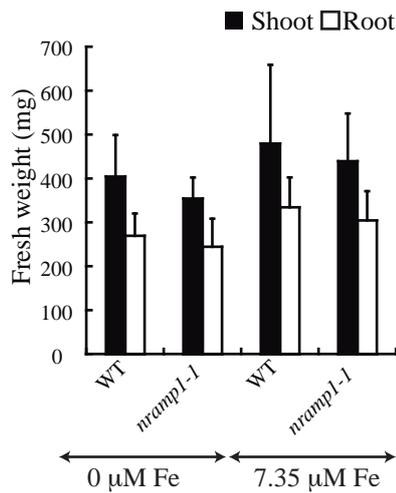
Supplemental Figure S5. MtNramp1-HA localization in the root. (A) Confocal microscopy localization of MtNramp1-HA in a cross section of a 28 dpi *M. truncatula* root transformed with a vector expressing *MtNramp1* under the regulation of its endogenous promoter. MtNramp1 position was determined using an Alexa 594-conjugated antibody (red). DNA and xylem was stained with DAPI (blue). (B) Optical image of the cross section. (C) Overlay of panels A and B. (D) Close-up of overlaid MtNramp1-HA localization in *M. truncatula* transformed roots (detected with an Alexa 594-conjugated antibody in red) and optical image. (E) Casparian strip localization (blue) detected with the berberine-aniline blue method. (F) Overlay of panels D and E. Scale bars represent 50 μm (panels A-C) or 10 μm (panels D-F).

SUPPLEMENTAL FIGURE S6

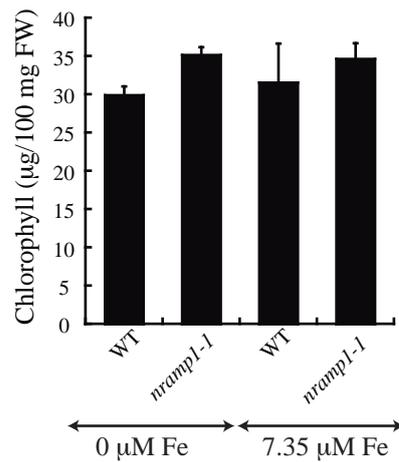
A



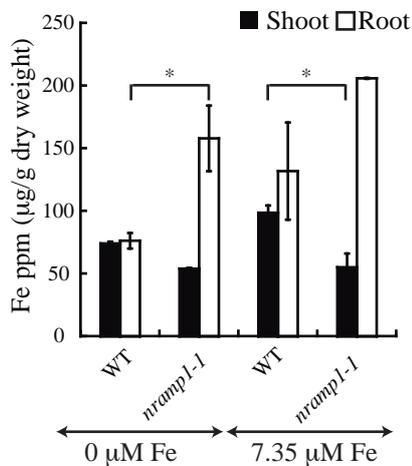
B



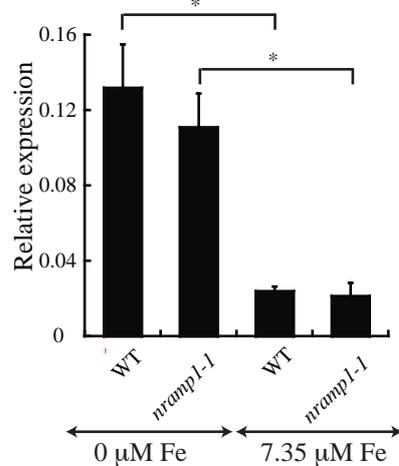
C



D

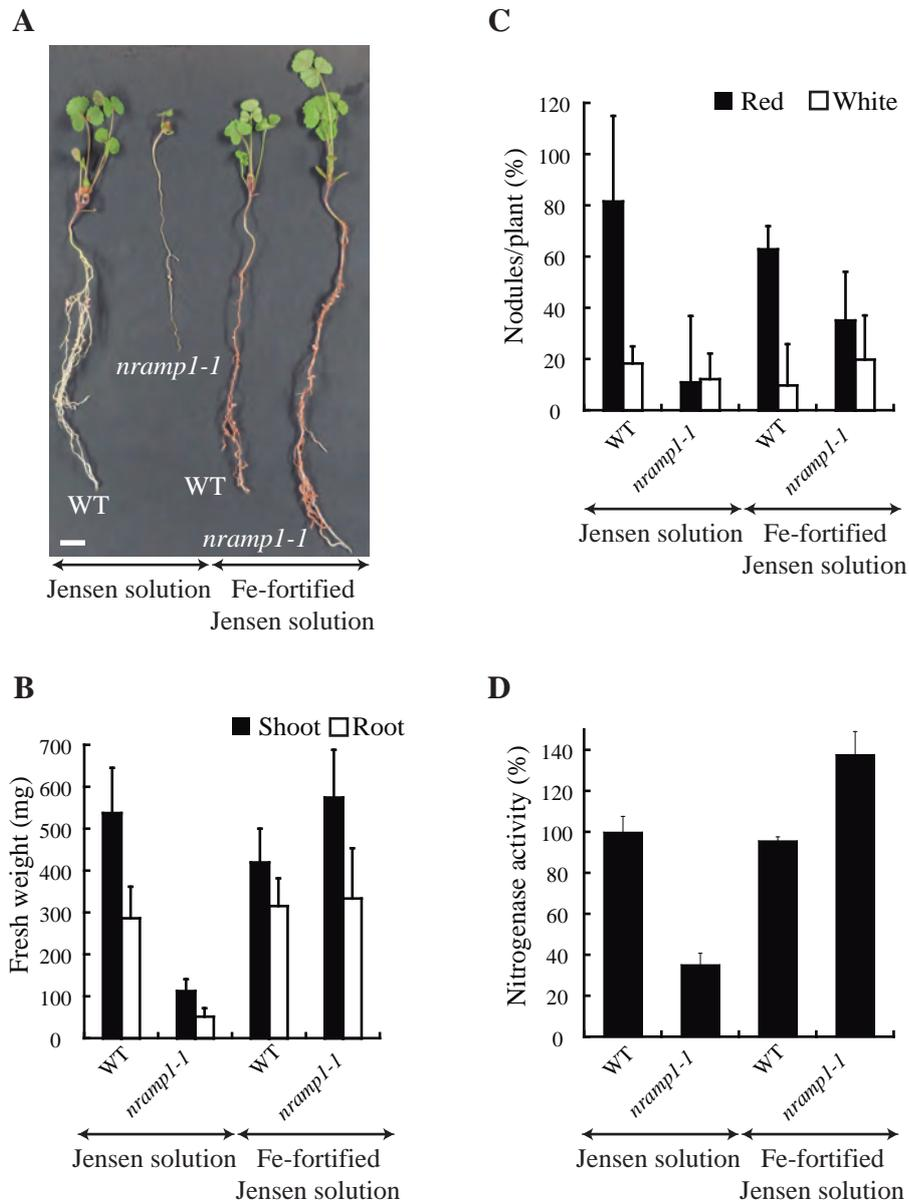


E



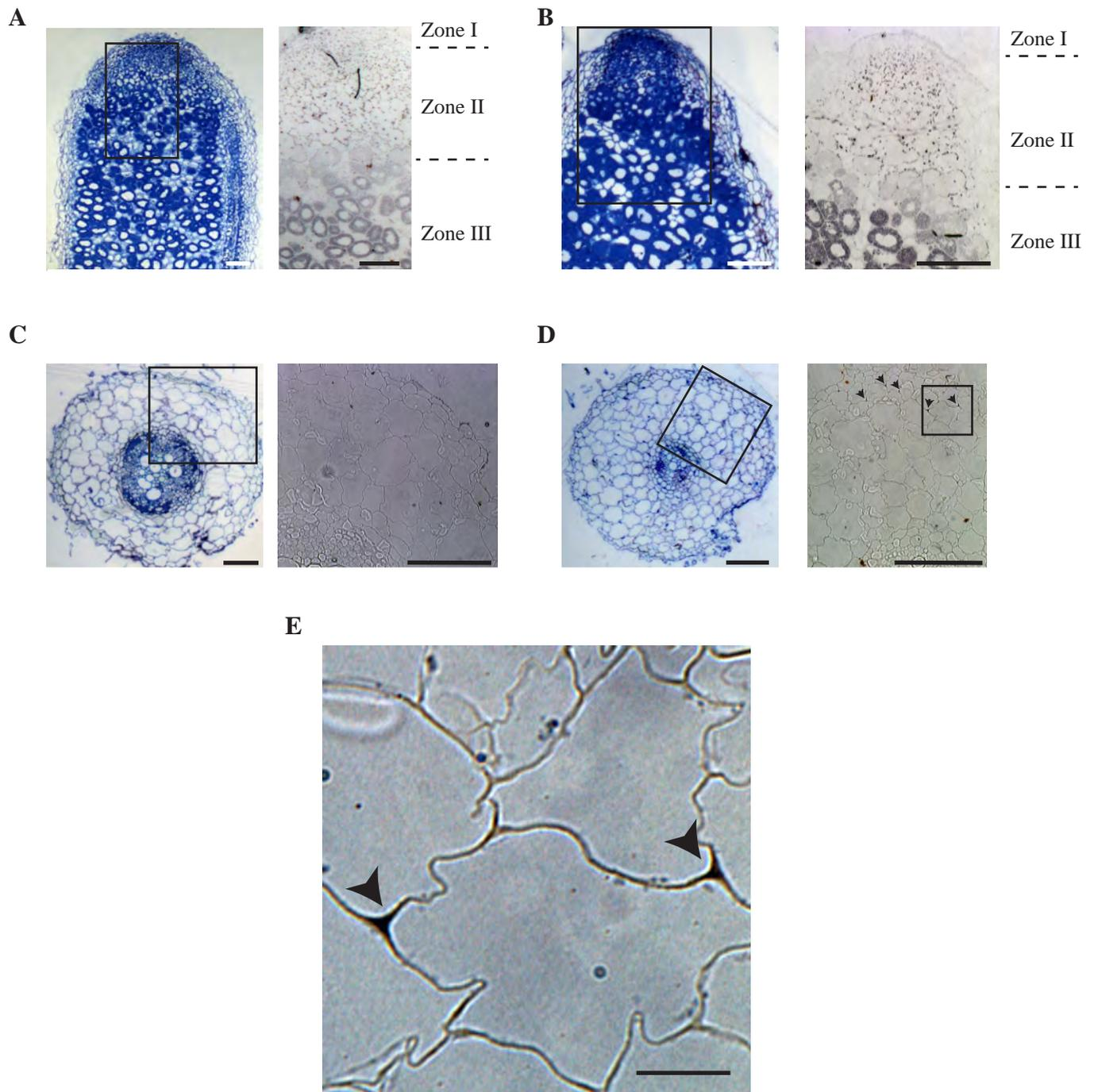
Supplemental Figure S6. Phenotype of *nramp1-1* under non-symbiotic conditions. (A) Growth of representative plants. Scale bar represents 1 cm. Fe concentrations in nutritive solutions used are indicated below. (B) Fresh weight of shoots and roots. Data are the mean \pm SE (n = 5 plants). (C) Chlorophyll content. Data are the mean \pm SE (n = 3 plants). (D) Iron content in roots and shoots of wild-type and *nramp1-1* plants under two different iron fertilization levels. Data are the mean \pm SE of two sets of five pooled plants. * indicates significant differences ($p \leq 0.05$). (E) *MtFRO1* expression in wild type and *nramp1-1* plants under two different iron fertilization levels. Data are the mean \pm SE of three independent experiments. * indicates significant differences ($p \leq 0.05$).

SUPPLEMENTAL FIGURE S7



Supplemental Figure S7. Iron complementation of *nramp1-1* phenotype. (A) Growth of representative plants. Scale bar represents 1 cm. (B) Fresh weight of shoots and roots. Data are the mean \pm SE (n = 8 plants). (C) Nodule number per plant. 100 % = 4.25 nodules/plant. Data are the average \pm SE (n=8-10 plants). (D) Nitrogenase activity in 28 dpi nodules. Acetylene reduction was measured in duplicate from two sets of five pooled plants. Data are the mean \pm SE. 100% = 61.17 nmol ethylene h⁻¹g⁻¹.

SUPPLEMENTAL FIGURE S8



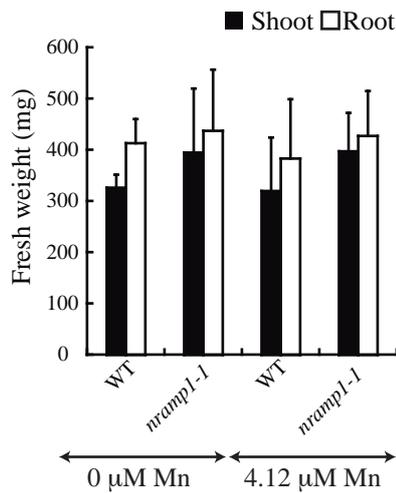
Supplemental Figure S8. Iron distribution in roots and nodules of wild type and *nramp1-1* plants. (A) wild type *M. truncatula* nodule and (B) *nramp1-1 M. truncatula* nodule. Left panels show reference sections stained with toluidine blue and methylene blue, the boxed regions represent the approximate area corresponding to the Perl-DAB-stained (right panel) which shows the iron distribution. Nodule zones are indicated. (C) Iron distribution in wild type *M. truncatula* root. Left panel shows a root section stained with toluidine blue and methylene blue, the boxed region represents the approximate area corresponding to the Perl-DAB-stained right panel. (D) Iron distribution in *nramp1-1 M. truncatula* root. Left panel shows a reference section stained with toluidine blue and methylene blue, the boxed region represents the approximate area corresponding to the Perl-DAB-stained right panel. Arrowheads indicate regions of iron accumulation. (E) Close-up view of Perl-DAB stained *nramp1-1* root (corresponding to the boxed area of the right panel in D). Arrowheads indicate regions of iron accumulation. Scale bars represent 100 μm (A-C, and left panel D), 50 μm (right panel D), or 10 μm (E).

SUPPLEMENTAL FIGURE S9

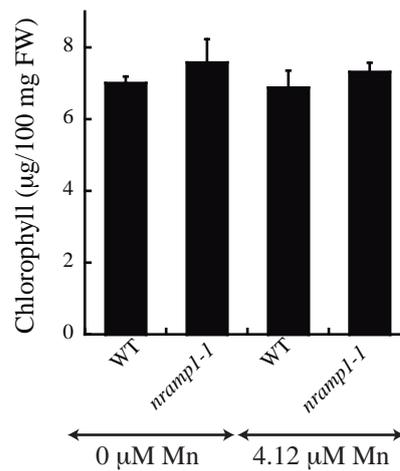
A



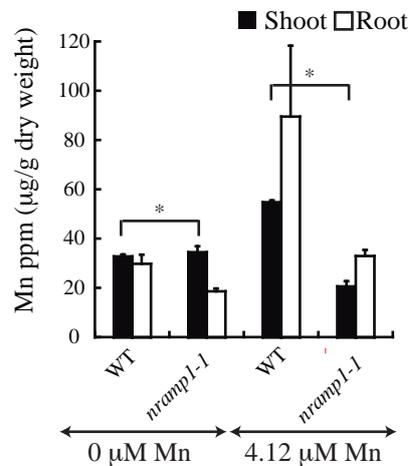
B



C

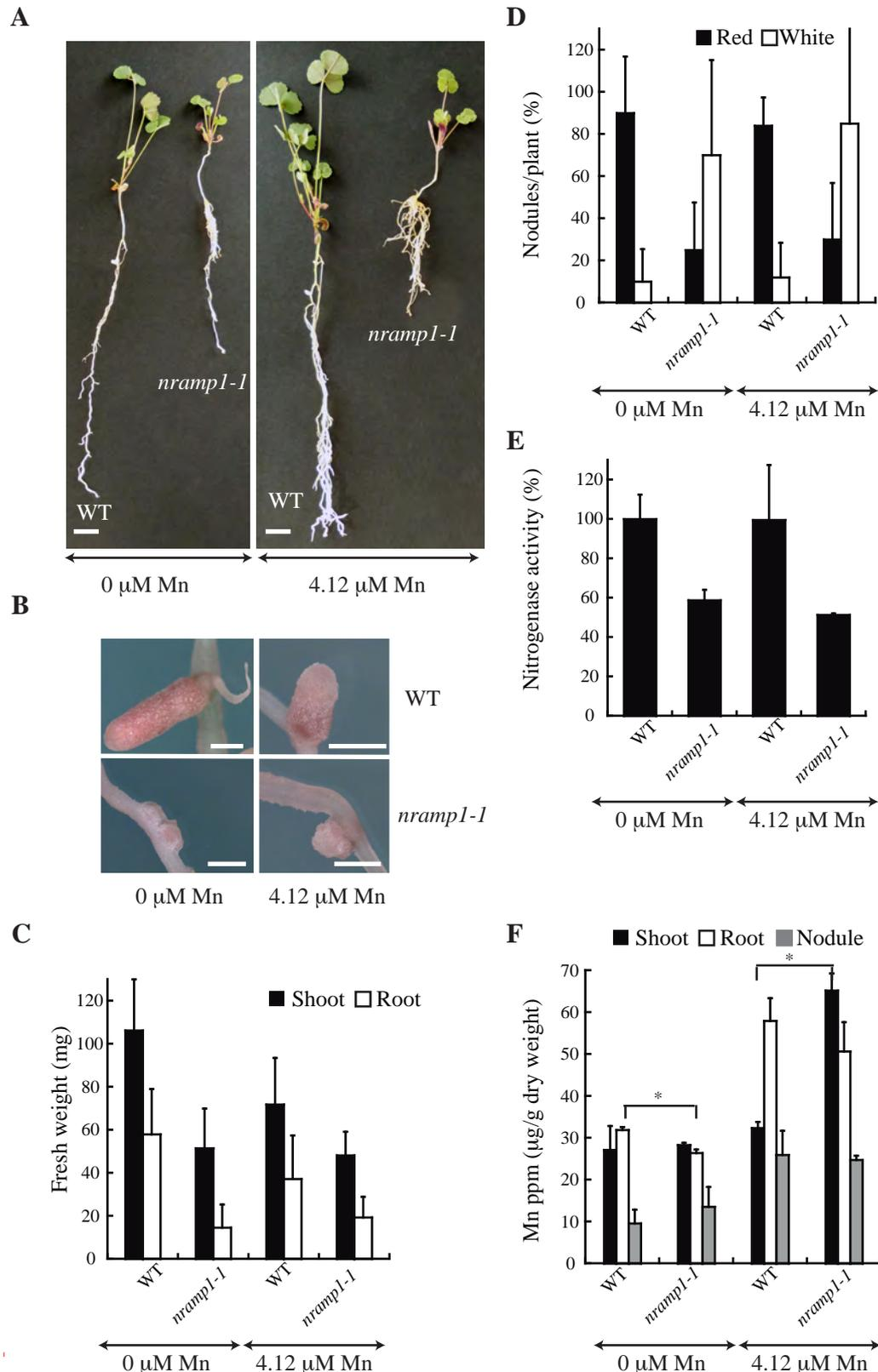


D



Supplemental Figure S9. Non-symbiotic phenotype of *nramp1-1* under Mn deficiency conditions. (A) Growth of representative plants. Scale bar represents 1 cm. Manganese concentrations in nutritive solutions used are indicated below. (B) Fresh weight of shoots and roots. Data are the mean \pm SE ($n = 5$ plants). (C) Chlorophyll content. Data are the mean \pm SE ($n = 3$ plants). (D) Manganese content in roots and shoots of wild-type and *nramp1-1* plants under two different manganese fertilization levels. Data are the mean \pm SE of two sets of five pooled plants. * indicates significant differences ($p \leq 0.05$).

SUPPLEMENTAL FIGURE S10



Supplemental Figure S10. Symbiotic phenotype of *nramp1-1* under two different Mn concentrations (A) Growth of representative plants. Scale bar represents 1 cm. (B) Close view of representative nodules of each *M. truncatula* line. Scale bar represents 1 mm. (C) Fresh weight of shoots and roots. Data are the mean \pm SE (n = 6-8 plants). (D) Nodule number per plant. 100 % = 4.21 nodules/plant. Data are the average \pm SE (n= 7 plants). (E) Nitrogenase activity in 28 dpi nodules. Acetylene reduction was measured in duplicate from two sets of five pooled plants. Data are the mean \pm SE. 100% = 26.69 nmol ethylene h⁻¹g⁻¹. (F) Mn content (ppm) in 28 dpi plants. Bars indicate the average \pm SE of two sets of 5 transformed plants. * indicates significant differences (p \leq 0.05).